

Finite Element Simulation of Cold Formed Steel Stiffened Zed Sections for Local, Distortional And Lateral Torsional Buckling

Yerudkar D S^a, Vesmawala G R^B

^AResearch Scholar, Sardar Vallabhbhai National Institute Of Technology, Surat-395007, Gujrat, India

^BAssistant Professor, Sardar Vallabhbhai National Institute Of Technology, Surat-395007, Gujrat, India

ABSTRACT: The aim of this paper is to explore the post-buckling behavior and ultimate strength of cold-formed steel (CFS) stiffened members in bending. The Finite Element (FE) models provide a supplementary tool to verify the design methods as well as to explore the buckling mechanism of cold formed steel members with various configurations. In this paper, the numbers of finite element models are established using ANSYS software for both stiffened and unstiffened elements. A particular emphasis has been given to the study of strength and behaviour of different cold formed steel zed sections with flange or web intermediate stiffeners. Cold formed steel members can be plain in simple applications, but if provided with flange or web stiffeners, their performance and resistance to local, distortional and lateral torsional buckling improves. The idea behind this paper is to use cold-formed steel members with modifying the shape rather than thickness to support load. Due to the relatively easy method of manufacturing, a large number of different configurations can be produced to fit the demands of optimized design for both structural and economical purposes.

Keywords: Cold Formed Steel, Z sections, intermediate stiffeners, buckling behaviour, bending.

I. INTRODUCTION

Cold-formed steel structures are steel structural products that are made by bending flat sheets of steel at ambient temperature into shapes which will support more than the flat sheets themselves. They have been produced for more than a century since the first flat sheets of steel were produced by the steel mills. Consumption rate of cold-formed steel products is growing steadily. The reasons behind the growing popularity of these products include their ease of fabrication, high strength/weight ratio and suitability for a wide range of applications. These advantages can result in more cost-effective designs, as compared with hot-rolled steel, especially in short-span applications [4]. However, in recent years, higher strength materials and a wider range of structural applications have caused a significant growth in cold-formed steel relative to the traditional heavier hot-rolled steel structural members. Cold-formed steel members have been widely used in building applications as the secondary cladding and purlin applications as well as the primary applications as beams and columns of industrial and housing systems. Cold-formed members can be produced in a wide variety of sectional profiles. The commonly used open cold formed sections are the “C” channels and the “Z” zed sections shown in Fig. 1. While plain sections are finding applications as secondary members, the sections are usually enhanced with flange end stiffeners (e.g. the lipped channels) and/or web stiffeners in primary structural applications [11, 20]. With stiffeners, the members benefit from a larger cross-sectional effective area and are therefore expected to become better able to resist local and overall buckling.

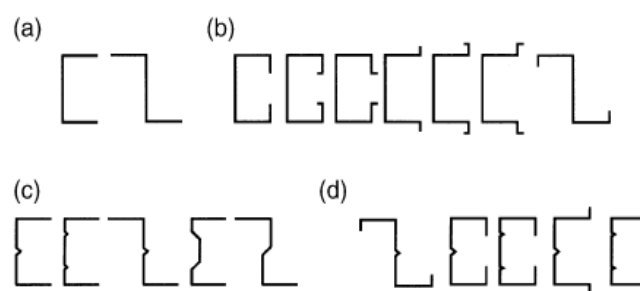


Figure 1: C and Z cold-formed sections (a) Plain sections; (b) Sections with flange stiffeners; (c) Sections with web stiffeners; (d) Sections with flange and web stiffeners.⁴⁵

II. FINITE-ELEMENT ANALYSIS

General

Finite-element analysis (FEA) of cold-formed steel structures plays an increasingly important role in engineering practice, as it is relatively inexpensive and time efficient compared with laboratory experiments, especially when a parametric study of cross section geometries is involved (Young and Yan 2002). Thus, numerical investigation based on the nonlinear finite-element method is an effective way to solve engineering problems. The key of such a numerical investigation is the validity of the finite element model. The material and geometric nonlinearities as well as the complex boundary conditions make it difficult to establish an accurate finite-element model. Several tools are available when considering the design of cold-formed sections such as testing, classical methods based on explicit solutions of the governing differential equations, finite-element method, and finite-strip method (Davies 2000). Among these methods, the finite-element method is used mostly because of its economy and time efficiency in dealing with both geometrical and material nonlinearities. The purpose of this paper is to develop accurate nonlinear finite-element models to study the buckling behavior of cold formed steel Z section beams for the applied loading conditions. The finite-element program ANSYS (2009) was used for the numerical analysis. Two types of Z sections were chosen 1) simple Z sections (Fig. 2 (i)) and 2) stiffened Z sections (Fig.2 (i) to (v)). The cross-section dimensions, material properties, and boundary conditions used in developing the FE models are as given in Table I&II, Table III, and Fig. 3 respectively. The Z sections of the models were based on the centerline dimensions of the cross sections together with the plate thickness and rounded corners. The length of the beams is taken as 3m constant for all the sections. The sections are chosen with variable H/B, H/t and B/t ratios (Ref. Table IV).

Table I: Geometric Properties for end stiffened Z sections (B=40)

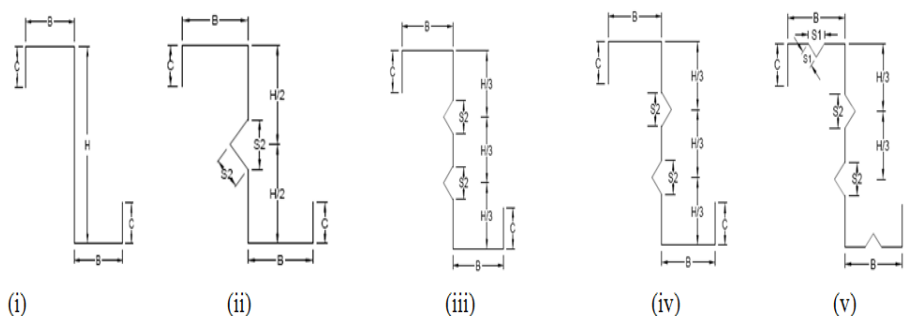
Sr. No.	H	B	C	T	Area	W	I _{yy} x10 ⁴	Z _{xx} x10 ³	Z _{yy} x10 ³
1	100	40	15	2	387	30.4	14.10	11.58	3.62
2	160	40	15	2	507	39.8	14.11	22.34	3.62
3	200	40	15	2	587	46.1	14.11	30.87	3.62
4	240	40	15	2	667	52.3	14.11	40.46	3.62
5	280	40	15	2	747	58.6	14.11	51.13	3.62

Table II: Geometric Properties for end stiffened Z sections (B=70)

Sr. No.	H	B	C	T	Area	W	I _{yy} x104	Z _{xx} x103	Z _{yy} x103
1	100	70	20	2	527	41.4	72.99	17.76	10.58
2	160	70	20	2	647	50.8	72.99	32.68	10.58
3	200	70	20	2	727	57.1	73.00	43.99	10.58
4	240	70	20	2	807	63.3	73.00	56.38	10.58
5	280	70	20	2	887	69.6	73.00	69.83	10.58

Table III: Material Properties

Property	Values
Modulus of elasticity (E)	2x10 ⁵ MPa
Shear modulus	0.769x10 ⁵ MPa for μ=0.3
Poisson's ratio	
(i) Elastic range	0.3
(ii) Plastic range	0.5
Unit mass of steel, (ρ)	7850 Kg/m ³
Coefficient of thermal expansion, (α _t)	12x10 ⁻⁶ /°C
Yield strength	250 MPa
Elongation	23%



Element Type and Mesh

A thin shell element (Shell181) was used to model the sections. This shell element is suitable for thin structures with large strain nonlinear capabilities, a large rotation, and large deflection. This is a four-node element with six degrees of freedom at each node. One of the most important aspects of FE modelling is to identify a suitable mesh size for the accurate modelling of the structural response. Finer meshes are generally preferred to obtain better predictions although there is in general guideline for such fineness, which largely depends on the type of structure and analysis involved. Thus performing a convergence study is a pre-requisite for finding a suitable mesh for any FE investigation. Although finer meshes generally provide better predictions, they make the whole process more expensive in terms of the computational time. A compromise is therefore needed between the required level of accuracy and the cost of a solution. Two different mesh sizes were used to simulate the load–deformation response of beams considered in the present study. Mesh sizes of approximately 10 mm x 10mm (length by width) for both flange and web elements were selected. The corresponding aspect ratios (length-to-width ratio) were 1.0 for both flange and web elements. A finer mesh of size 5 mm x 5 mm was implemented for the corners due to their importance in transferring the stress from the flange to the web. Typical finite-element meshes of the channels are shown in Fig. 4 for applied loading conditions.

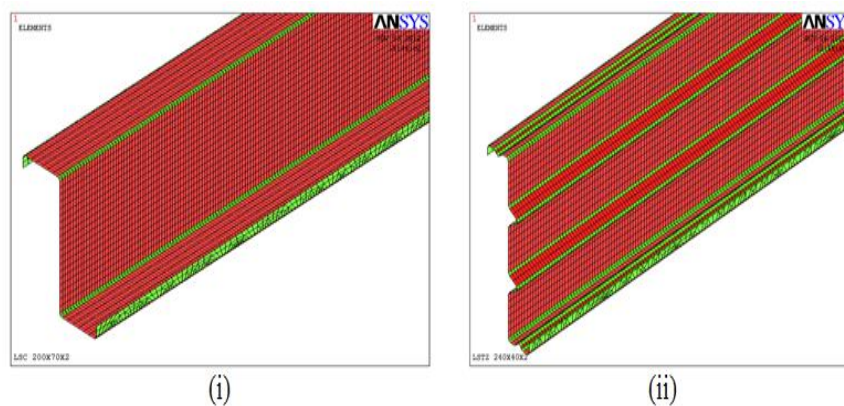


Figure 4: Meshing of the Simple and Stiffened Zed Section

Basic Aspects of FE Modelling—Boundary Conditions and Analysis Technique

In the present study, the elastic linear analysis technique using the BUCKL command [1] was employed to obtain the Eigenmodes, which were subsequently used to represent initial geometric imperfections. A ‘Block Lanczos’ method was used, to simulate the actual load–deformation response of the beams. A nonlinear FE analysis by incorporating material nonlinearity was performed using the Newton–Raphson iteration method. The simulation of boundary and connection conditions is the most difficult part in FE models. The boundary condition was taken as simply supported at both the ends as shown in Fig.3 (a). The loading was taken as symmetrical concentrated point load P at equidistant from both the supports.

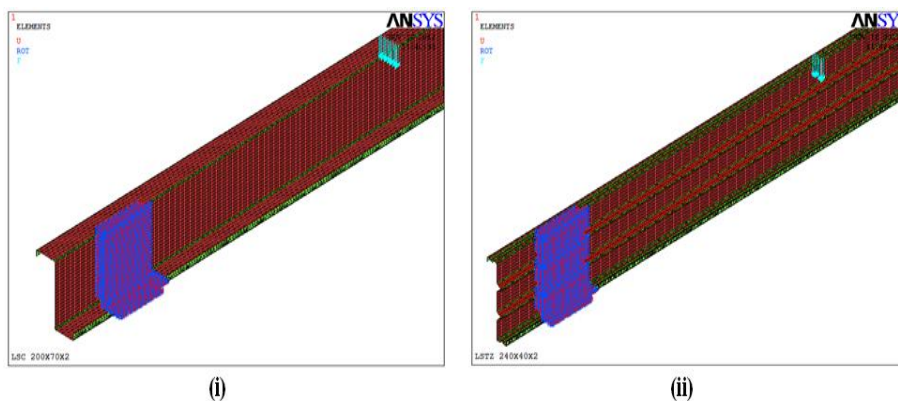


Figure 5: Simple Support at Ends and Point Load at One Third Spans

In the FEA the type of loading was taken as ramped load. During the experimental validation the sections would be bolted to the load transfer blocks. To fulfill this assumption, the node coupling method was used in FEA; in the region where the sections will be connected to the load transfer blocks. The nodes at the x, y

and z coordinates in the region were coupled together by all degrees of freedom. For the regions where the load was applied through the bearing plates, the same technique was implemented for the range of 15 cm wide web and bottom flanges connected to the bearing plates as shown in Fig. 5. The rest of the nodes were free to translate and rotate in any direction under the applied load.

Geometric Imperfections

Geometric imperfections are inseparable property of real steel members, with the potential to significantly influence their structural behaviour. When performing an FEA to predict the ultimate load, the model should, in general, include both local and global initial imperfections. The nonlinear effects arising from geometric and material nonlinearity were included using the 'NLGEOM' option and 'PRSTRES' command respectively as stated in ANSYS [1]. All the beams are treated as geometrically nonlinear static problems involving buckling, where the load-displacement response shows a negative stiffness making the structure 'unstable' after reaching the peak load. ANSYS [1] offers several techniques to analyze this type of problem and among the available options, the 'Newton Raphson method' was chosen because of its simplicity and widespread use in similar applications. Despite the importance of initial geometrical imperfections, there are no general guidelines for their specification. Predictions are normally conducted by either modeling the structure with an assumed initial out-of-plane deflection or by using assumed small transverse forces. Accurate knowledge of distribution, shape and magnitude of imperfections is a prerequisite for numerically simulating the response of a structural member. In the absence of suitable measured data, the magnitude and distribution of imperfections (which is likely to be a complex function of the rolling and fabrication process, material strength and geometrical properties of the cross-section) must be predicted.

Material Modeling

Non-linearity in the material of section was modeled with Von Mises yield criteria and isotropic hardening. A stress-strain curve is given as an input in FEM programming to define the stress-strain relationship of material. The initial slope of the curve is taken as the elastic modulus (E) of the material. All other components were modeled as elastic, i.e. the elastic modulus was equal to 200 GPa and the Poisson's ratio to 0.3. Residual stresses and cold-work due to forming (where the apparent yield stress in the corners is increased) were ignored.

Failure Modes

The failure mode of the cold-formed steel zed sections subjected to ultimate strength highly depends on the loading conditions. The most commonly used technique, employing Eigenmodes to define the initial geometry of a structure, was adopted in the present work. The Eigenmodes were obtained from elastic buckling analyses of the beam models. The worst imperfection shape, resulting in the greatest reduction in load-carrying capacity, often relates to the lowest Eigenmode, though it is not always the case. In this study, each of the first Eigenmode was used individually to investigate the effect of imperfection distribution on load-deformation response. Fig. 6 shows some typical Eigenmodes and Fig. 7 shows the typical failure modes obtained from the nonlinear FEA, at the ultimate loads attained for all the cross-section types considered.

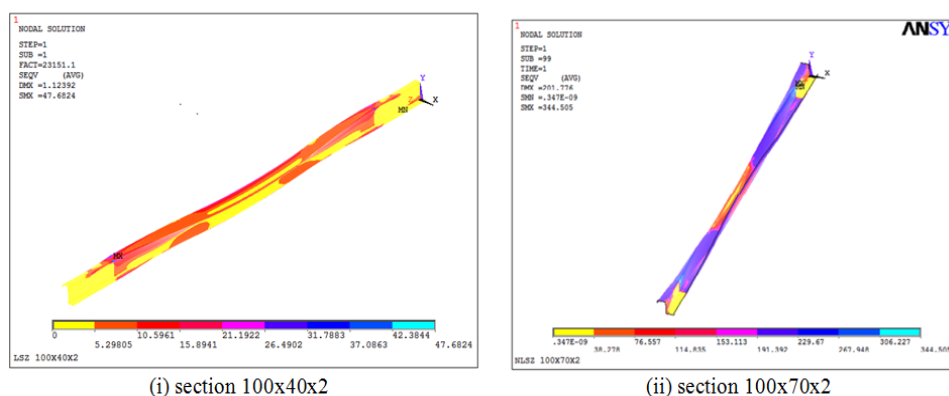


Figure 6: 1st Buckling Modes

III. RESULTS AND DISCUSSION

The results of Eigenvalue buckling analysis in terms of linear buckling loads and first buckling mode are extracted and used further in nonlinear buckling analysis. Table IV shows the Eigenvalue buckling loads in the studied sections. The maximum stresses and the deflections at the ultimate load of the sections are extracted

from the nonlinear analysis results. Table V&VI shows the comparative study of the maximum stresses and the maximum deflection in the simple and stiffened sections. The values of stresses and deflections considered under stiffened column are the maximum of all types of stiffened zed sections considered in the study.

Table IV: Eigen value Buckling Loads in sections

Sr. No	Section	H/B Ratio	H/t Ratio	B/t Ratio	Linear Buckling Load (N)					
					Simple Z section	Only one Stiffener in Web	Two stiffeners in web	Stiffeners both in web and flange		
								Opp. side of web	Same side of web	
- ve x co-ordinate side	+ ve x co-ordinate side									
1	100x40x2	2.5	50	20	5977	5242	5328	4876	4959	5140
2	100x70x2	1.4	50	35	18169	18165	18246	19189	19446	19660
3	160x40x2	4	80	20	9783	7811	8086	7278	7538	8028
4	160x70x2	2.3	80	35	19028	26215	26366	29430	30470	30726
5	200x40x2	5	100	20	9539	9024	4547	8312	8789	8327
6	200x70x2	2.8	100	35	17365	32851	32782	36508	38009	37928
7	240x40x2	6	120	20	12969	9671	10486	9011	9512	10438
8	240x70x2	3.4	120	35	16235	32022	31137	35528	36919	35545
9	280x40x2	7.0	140	20	13179	11509	12131	11207	11988	12127
10	280x70x2	4.0	140	35	15390	27647	26713	31877	32850	30544

Table V: Maximum Stresses in sections

Sr. No	Section	H/B Ratio	H/t Ratio	B/t Ratio	Maximum Stress (N/mm ²)	
					Simple	Stiffened
1	100x40x2	2.5	50	20	255	241
2	100x70x2	1.4	50	35	344	343
3	160x40x2	4	80	20	265	294
4	160x70x2	2.3	80	35	Unconverged	356
5	200x40x2	5	100	20	299	240
6	200x70x2	2.8	100	35	282	374
7	240x40x2	6	120	20	295	310
8	240x70x2	3.4	120	35	Unconverged	369
9	280x40x2	7.0	140	20	296	288
10	280x70x2	4.0	140	35	Unconverged	289

Table VI: Maximum Deflection in sections

Sr. No	Section	H/B Ratio	H/t Ratio	B/t Ratio	Maximum Deflection (mm)	
					Simple	Stiffened
1	100x40x2	2.5	50	20	55	40
2	100x70x2	1.4	50	35	201	180
3	160x40x2	4	80	20	16	71
4	160x70x2	2.3	80	35	Unconverged	212
5	200x40x2	5	100	20	37	28
6	200x70x2	2.8	100	35	51	207
7	240x40x2	6	120	20	27	66
8	240x70x2	3.4	120	35	Unconverged	212
9	280x40x2	7.0	140	20	18	33
10	280x70x2	4.0	140	35	unconverged	195

Comparative Graphical Representation of Deflection and Stresses in the Simple and Stiffened zed sections The load v/s deformation and load v/s stress results of the simple and stiffened zed sections shows that; the behavior of the simple and stiffened sections is different with respect to various H/B, H/t and B/t ratios. A typical behavior for a beam as a result of changing the shape of the imperfection distribution is shown in Fig. 8 and 9.

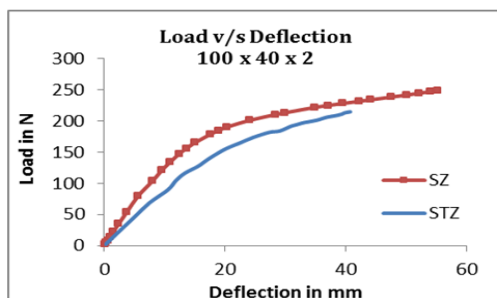


Figure 8: Load v/s Deflection curves

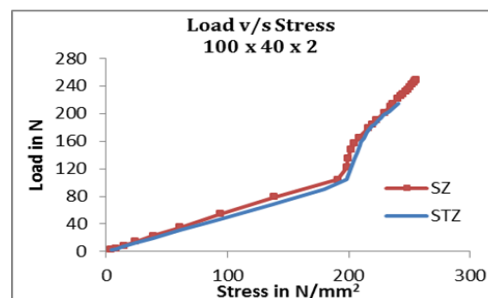


Figure 9: Load v/s Stress curves

From the Finite Element analysis results of the cold formed steel zed section flexural members, having variable H/B, H/t and B/t ratios following results have been drawn:

- After addition of intermediate stiffeners, the linear buckling loads are reducing in sections having $B/t \leq 20$; whereas it is increasing for the sections having $B/t > 20$.
- For section having $H/t = 50$, the maximum stresses are reduced slightly.
- For sections having $B/t \geq 20$ but $H/t \leq 100$ the maximum deflection is decreased and stresses are increased.
- In three sections 160x40x7, 270x70x2 and 280x70x2, rigid body motion has occurred when net section yielding has occurred resulting in large displacements of small increments of load or when buckling has occurred. Problems are unconverged because of rigid body motion or buckling. The slope of time history curve for the node having maximum stress is approaching to zero when problems are unconverged.
- In load versus stress graphs, it is observed that there is sudden change in slope of graph in between 150 to 200 N/mm² stress. It shows that theoretical critical local buckling stress is reached within this range of stress. The member is continued to carry additional load by means of the redistribution of stress after local buckling occurs. This is well-known phenomenon called post buckling strength of plates. The post buckling strength may be several times larger than the strength determined by critical local buckling stress.

IV. CONCLUSION

From the above results it is to be concluded that:

- The provision of curved groove stiffeners in both web and flange are suitable for the sections having $B/t > 20$ and $H/t \leq 100$
- The unconverged sections should be converged by stabilization. If not converged, the provision of stiffeners should be changed.

Notation

The following symbols are used in this paper:

μ = Poisson's ratio;

B = overall width of flange;

C = width of end stiffener;

E = young's modulus of elasticity;

FEM = finite-element method;

f_y = yield stress;

H = overall depth of section;

I_{yy} = moment of inertia about the minor axis of the cross section;

L = length of specimen;

P = concentrated point load;

R = centerline corner radius of specimen;

T = thickness of section;

Z_{xx} = section modulus about the axis perpendicular to the plane of the cross section;

Z_{yy} = section modulus about minor axis of the cross section.

REFERENCES

- [1]. ANSYS (2009). User's manual, revision 12.1, Swanson Analysis System.
- [2]. Ashrafa, M. Gardner, L. Nethercot, D. A. (2006), "Finite element modelling of structural stainless steel cross-sections." *J.Thin-Walled Structures*, 44, 1048–1062.
- [3]. Dinis P.B., Camotim D. (2010), "Local/distortional mode interaction in cold-formed steel lipped channel beams." *J.Thin-Walled Structures*, 48, 771–785.
- [4]. El-Sheikh, A.I. El-Kassas, E.M.A. Mackie, R.I. (2001), "Performance of stiffened and unstiffened cold-formed channel members in axial compression." *J.Engineering Structures*, 23, 1221–1231.
- [5]. I S 801. (1975), "Indian Standard Specification for Cold Formed Steel Structures".
- [6]. Li, L. Chen, J. (2008), "An analytical model for analysing distortional buckling of cold-formed steel sections." *J.Thin-Walled Structures*, 46, 1430–1436.
- [7]. Macdonald, M. Heiyantuduwa, M. A. Rhodes, J. (2008), "Recent developments in the design of cold-formed steel members." *J.Thin-Walled Structures*, 46, 1047–1053.
- [8]. Magnucka-Blandz, E. Magnucki, K. (2011), "Buckling and optimal design of cold-formed thin-walled beams: Review of selected problems." *J.Thin-Walled Structures*, 49, 554–561.
- [9]. Nandini, P. Kalyanaraman, V. (2010), "Strength of cold-formed lipped channel beams under interaction of local, distortional and lateral torsional buckling." *J.Thin-Walled Structures*, 48, 872–877.
- [10]. Nuno, S. Dinar, C. (2006), "Local-plate and distortional postbuckling behavior of cold-formed steel lipped channel columns with intermediate stiffeners." *J. Structural Engineering*, 132, 529–540.
- [11]. Osama, B. (2009), "A cost-effective design procedure for cold-formed lipped channels under uniform compression." *J.Thin-Walled Structures*, 47, 1281–1294.
- [12]. Piecorak, E. Piekarczyk, M. (2007), "Analysis of the post-buckling behavior of a purlin built from thin-walled cold-formed C profile." *J.Thin-Walled Structures*, 45, 916–920.

- [13]. Ren, W. Fang, S. Young B. (2006), "Analysis and design of cold-formed steel channels subjected to combined bending and web crippling." *J.Thin-Walled Structures*, 44, 314–320.
- [14]. Ren, W. Fang, S. Young B. (2006), "Finite-element simulation and design of cold-formed steelchannels subjected to web crippling." *J. Structural Engineering*, 132, 1967-1975.
- [15]. Schafer, B. W. Pekoz, T. (1999), "Laterally braced cold-formed steel flexural members with edge stiffened flanges." *J. Structural Engineering*, 125,118-127.
- [16]. Schafer, B. W. Pekoz, T., (1998) "Cold-formed steel members with multiple longitudinal intermediate stiffeners." *J. Structural Engineering*, 124.
- [17]. Schafer, B. W. Sarawit, A. Peköz, T. (2006), "Complex edge stiffeners for thin-walled members." *J. Structural Engineering*, 132, 212-226.
- [18]. Schafer, B.W. Li, Z. Moen, C.D. (2010), "Computational modeling of cold-formed steel." *J.Thin-Walled Structures*, 48, 752–762.
- [19]. Wang, H. Zhang, Y. (2009), "Experimental and numerical investigation on cold-formed steel C-section flexural members." *J. Constructional Steel Research*, 65, 1225-1235.
- [20]. Xiao-ting, C. Zhi-ming. Long-yuan, L. Roger, K. (2006), "Local and distortional buckling of cold-formed zed-section beams under uniformly distributed transverse loads." *International Journal of Mechanical Sciences*, 48, 378–388.
- [21]. Young B., Yan J. (2004), "Numerical investigations of channel columns with complex stiffeners—Part I: Parametric study and design." *J.Thin-Walled Structures*, 42, 883–893.
- [22]. Young, B. (2008), "Research on cold-formed steel columns." *J.Thin-Walled Structures*, 46 731–740.
- [23]. Young, B. Yan J. (2004), "Numerical investigation of channel columns with complex stiffeners—Part II: parametric study and design." *J.Thin-Walled Structures*, 42, 895–909.
- [24]. Yu, C. Schafer, B.W. (2007), "Simulation of cold-formed steel beams in local and distortional buckling with applications to the direct strength method." *J. Constructional Steel Research*, 63, 581–590.
- [25]. Yu, W.W. (1985), "Cold –formed steel structures." John Wiley and Sons, New York.